

Sachdev-Ye-Kitaev model: Non-self-averaging properties of the energy spectrum

Richard Berkovits

Department of Physics, Jack and Pearl Resnick Institute, Bar-Ilan University, Ramat-Gan 52900, Israel

The short time (large energy) behavior of the Sachdev-Ye-Kitaev model (SYK) is one of the main motivations for the growing interest garnered by this model. True chaotic behavior sets in at the Thouless time, which can be extracted from the energy spectrum. In order to do so, it is necessary to unfold the spectrum, i.e., to filter out global tendencies. Using a simple ensemble average for unfolding results in a parametrically low estimation of the Thouless energy. By examining the behavior of the spectrum as the distribution of the matrix elements is changed into a log-normal distribution it is shown that the sample to sample level spacing variance determines this estimation of the Thouless energy. Using the singular value decomposition method, SVD, which filters out these sample to sample fluctuations, the Thouless energy becomes parametrically much larger, essentially of order of the band width. It is shown that the SYK model is non-self-averaging even in the thermodynamic limit which must be taken into account in considering its short time properties.

I. INTRODUCTION

The interplay between disorder and interactions in quantum systems has been a central theme in condensed-matter physics for the last half century. Recently the Sachdev-Ye-Kitaev (SYK) model [1, 2], has garnered much interest in the fields of quantum gravity and quantum field theory [3, 4]. A key feature of the model is that it follows random matrix theory (RMT) behavior, as is manifested in the chaotic behavior of its energy spectrum.

The SYK model first appeared in the context of spin liquids [1] and then in string theory [5] and quantum gravity [4]. The SYK model is known to be chaotic [6–8], showing a Wigner-like behavior of the energy spectra. Once the SYK model is perturbed by a single-body random term which mimics diagonal disorder in the Anderson model [9–15], or several SYK dots are coupled by single-body random terms [16–20], a transition from metallic (chaotic) to insulating behavior occurs which leads to a Wigner to Poisson crossover of the statistical properties of the spectra.

While studying nuclear and condensed-matter systems it became clear that many physical systems exhibit universal behavior at long times (short energy scales) [21–26]. Nevertheless, universality may break at shorter times (large energy scales) for which a particle had no time to sample the entire phase space of the system and its behavior depends on local non-universal features [27]. Thus, in the context of disordered metals the scale for which the metallic spectrum deviates from the universal behavior is known as the Thouless energy, $E_{Th} = \hbar D / \tilde{L}^2 = g \Delta$ (D is the diffusion constant, \tilde{L} is the linear dimension, g is the dimensionless conductance, Δ the average level spacing) and the Thouless time $t_{Th} = \hbar / E_{Th} = \tilde{L}^2 / D$.

The question whether an analogue of the Thouless energy manifests itself in the SYK model has surfaced in Ref. 6 where García-García and Verbaarschot have studied (among other things) the variance of the number of levels as a function of the size of an energy window E , denoted by $\langle \delta^2 n(E) \rangle$ (where $\langle \dots \rangle$ represents an ensemble

average and $n(E)$ is the number of levels within E). A departure from the RMT behavior is apparent above a certain value of E , which quite naturally was identified with the Thouless energy. Moreover, at larger energy windows, the number variance adopts a quadratic form $\langle \delta^2 n(E) \rangle = a + b(n(E))^2$. Evidence for the Thouless energy has also been seen for other measures such as off-diagonal expectation values [28]. In Ref. 19 the origin of the Thouless energy for the SYK was identified as the relaxation of modes prevailing at shorter scale. For disordered metals these modes are known as the diffusion modes. For SYK it was suggested that similar modes can be constructed, where the number of such modes is connected to the number of independent interaction terms in the SYK model which is much smaller than the size of the Hilbert space. This leads to an energy scale which determines the Thouless energy. Thus, the energy scale for the departure of the SYK model level number variance from the RMT prediction is determined by the scale of the sample to sample fluctuations of the ensemble.

For a single disordered realization of the SYK model all the terms have just a single variance scale, which is well behaved (box or Gaussian) and therefore the origin of the additional energy scale determining the Thouless energy is not obvious. As noted recently by Jia and Verbaarschot [30] this deviation from RMT behavior has its root in large scale sample to sample fluctuations of the spectrum. They attribute these fluctuations to the relatively small number of independent random variables contributing to the SYK Hamiltonian. When these small number of long-wavelength sample to sample fluctuations are parameterized by terms of Q-Hermite orthogonal polynomials and removed from the spectrum of a particular realization a pure RMT behavior is retained up to a very large energy scale.

The influence could be quantified [30] by estimating the energy scale for which the small number of independent random variables will change the number variance. Using the notation for the complex SYK (CSYK) half-filled model defined in the next section, where L is the number of sites, the size of the Hilbert space is $\binom{L}{L/2} \sim 2^L$. The

number of independent variables is $\binom{2L}{4} \sim L^4$ leading to a variance of L^{-2} in any observable. Thus one expects the number of levels n to deviate significantly $O(1)$ from RMT predictions on a scale of $n \sim L^2$. A similar result emerges from the calculation in Ref. 19 where the coefficient b in the number variance was estimated as $b \sim L^{-4}$ thus becoming significant at $n \sim L^2$.

Although the deviation from RMT is shifted to larger n as the system size L increases, the proportion of levels following RMT predictions out of the the total number of states goes to zero as $L^2/2^L$. On the other hand, one would expect that after filtering out long wavelength sample to sample fluctuations the RMT behavior will be followed for a finite portion of the spectrum. Thus, one expects the Thouless energy to crucially depend on whether one simply averages over an ensemble or takes into account the single sample adjustments. This is a hallmark of a non-self-averaging system [31]. The number variance for the ensemble average is different than the number variance adjusted to a particular sample.

Hence, the energy scale for which the spectrum departs from the RMT predictions crucially depends on the the unfolding, i.e., the method by which the averaged over the density of states is performed. Estimating the local density of states by a simple ensemble average will give a different value than an unfolding method that is able to take into account sample specific global behavior of the spectrum. In recent studies it has been shown that [32–38], these sample specific long ranged features of the spectrum can be identified by the singular value decomposition (SVD) procedure. As detailed below, similar in a sense to Fourier transform, SVD actually reconstructs the energy spectrum of each realization by a sum over a series of SVD amplitudes multiplied by the corresponding SVD mode. Unlike the Fourier transform, the amplitudes of the SVD are identical for all realizations while the modes are realization specific. Generally, plotting the amplitudes from large to small (known as a Scree plot) shows that the largest amplitudes (usually $O(1)$ modes) are orders of magnitude larger than the rest, while the following modes amplitudes obey a power law. The largest amplitudes modes depict the very long wave length behavior of the spectra, while the modes whose amplitudes follow a power law capture the shorter range properties. Thus SVD is a very natural method to examine the SYK spectrum behavior, and uncover the realization specific universal properties of the spectrum.

One may conclude that there are two possible energy scales for the deviation of the spectrum of the SYK model from RMT predictions. The first is the energy scale corresponding to the deviation from the ensemble average, which in self averaging systems such as disordered metals is the Thouless energy. The second energy scale corresponds to the deviation from RMT when the sample to sample long-wavelength fluctuations are removed from the spectrum. This sample specific parameterization of these long range behavior can be done using Q-Hermite orthogonal polynomials [30] or by SVD [32–38], or prob-

ably by other method. The energy scale of these fluctuations is another relevant energy scale which for self-averaging systems such as disordered metals is equivalent to the Thouless energy obtained from the ensemble average [36]. For a non-self-averaging system such as the SYK model, these two energy scales are not equal, and for clarity we will retain the notation of Thouless energy, E_{Th} , for the case where the spectrum is unfolded by a local average over all realizations, while the realization adjusted Thouless energy E_{Th^*} is obtained using a realization adapted unfolding method.

Here we will show that one can tweak the behavior of the CSYK model to a more non-self-averaging behavior by changing the distribution of the off-diagonal to a log-normal distribution. Thus it is possible to enhance the sample to sample fluctuations and study its influence on E_{Th} and E_{Th^*} . Such a wide distribution was not previously considered for the SYK model and should help to clarify the divergence of E_{Th^*} from E_{Th} .

The paper is arranged as follows: CSYK is defined in Sec. II. Corroborating the expected behavior for short range energy scales is performed in Sec. III. The universal statistics 4-fold symmetry as function of the system size is observed. In Sec. IV long range energy scales are probed by the number variance. The spectrum is unfolded by using the local ensemble averaged level spacing. RMT predictions hold only up to E_{Th} , which becomes smaller as the log-normal distribution acquires a thicker tail towards larger values. Above E_{Th} the variance increases quadratically as function of the number of levels in the energy window. In Sec. V we switch to the SVD analysis. This analysis reveals that each realization has a distinct long-range correlated level spacing structure. Thus, one should adapt the unfolding for each realization. After a realization adapted unfolding the number variation follows the RMT prediction for much larger energy scales, i.e., $E_{Th^*} \gg E_{Th}$. Actually, E_{Th} could be estimated from the sample to sample variance in the level spacing. In Sec. VI these results are discussed in the limit of large CSYK systems, showing the in the thermodynamic limit the SYK is non-self-averaging.

II. COMPLEX SYK MODEL

Here we use the the complex spinless fermions version of the SYK model given by the following Hamiltonian:

$$\hat{H} = \sum_{i>j>k>l}^L V_{i,j,k,l} \hat{c}_i^\dagger \hat{c}_j^\dagger \hat{c}_k \hat{c}_l, \quad (1)$$

the couplings $V_{i,j,k,l}$ are complex numbers, where the real and imaginary components are independently drawn from an identical distribution. We study here two different distribution: The first is a box distribution between $-L^{-3/2}/2 \dots L^{-3/2}/2$, where L is the number of sites.

The second distribution is the log-normal distribution

$$P(V) = (A/|V|)e^{\frac{-\ln^2(|V|/V_{\text{typ}})}{2p \ln(V_{\text{typ}}^{-1})}}, \quad (2)$$

with $V_{\text{typ}} \sim K^{-\gamma/2}$, K is the size of the Hilbert space, A a normalization and γ , p are parameters. For simplicity here we shall set $p = 0.5$, while γ is varied [39]. Thus, the log-normal distribution becomes wider and more skewed as γ increases. The number of fermions is conserved and we considered the $N = L/2$ sector for even L and $N = (L + 1)/2$ sector for odd L . Resulting in a Hilbert space size of $K = \binom{L}{N}$, and a matrix size of $K \times K$.

III. SHORT ENERGY SCALES

As a first step we would like to probe the nearest neighbor level spacing statistics of the CSYK box distributed in order to establish the extended regime of this model. One expects that in the extended regime short energy scales (long times) follow the Wigner statistics. The short energy scale statistics is revealed by the ratio statistics, defined as:

$$r = \langle \min(r_n, r_n^{-1}) \rangle, \quad (3)$$

$$r_n = \frac{E_n - E_{n-1}}{E_{n+1} - E_n},$$

where E_n is the n -th eigenvalue of the Hamiltonian and $\langle \dots \rangle$ is an average over an ensemble of different realizations of disorder and half of the eigenvalues around the middle of the band. For the Wigner distribution $r_s \cong 0.5307$ for the GOE symmetry, $r_s \cong 0.5996$ for GUE and $r_s \cong 0.6744$ for GSE. [40].

An interesting behavior emerges for the CSYK. It is known that as a consequence of the symmetries of the SYK model, the spectrum of Eq. (1) shows statistics which depends on L [6–8]. For $L \bmod 4 = 0$ the statistics are GOE, For $L \bmod 4 = 2$ the statistics are GSE, and for $L \bmod 4 = 1, 3$ the statistics are GUE. This is indeed seen in Fig. 1 where r_s averaged over the middle half of the energy spectrum, for different sizes $L = 8, 9, 10, 11, 12, 13, 14, 15, 16, 17$ and number of fermions $N = 4, 5, 5, 6, 6, 7, 7, 8, 8, 9$ is plotted. In all cases we exactly diagonalize the corresponding $K \times K$ matrix and average over 3000 realizations of disorder (except for the largest size for which only 100 realization were computed). It can be seen that the expected 4-fold symmetry is followed.

Concentrating on the $L = 16$ with $N = 8$ systems, we investigate the role played by changing the distribution from the box distribution to a log-normal. Setting $p = 0.5$ and increasing γ we sweep through the values $\gamma = 1, 1.5, 2, 2.5, 3, 4, 5$. For all these values $r_s \cong 0.5307 \pm 0.001$. Thus, GOE universal behavior on short energy scales is perfectly followed.

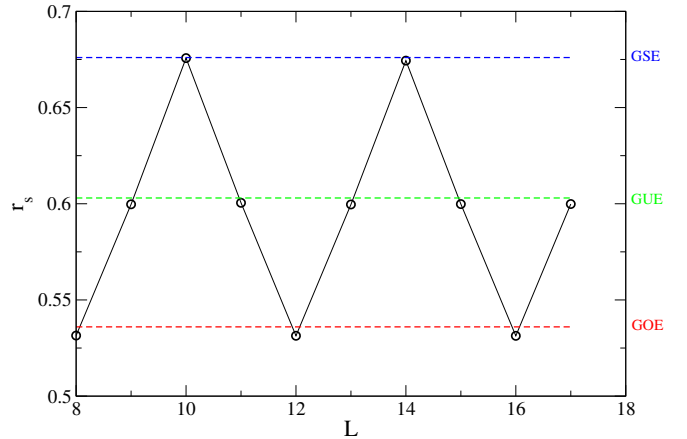


FIG. 1. The nearest neighbor level spacing statistics as manifested in the behavior of the ratio statistics r_s for different system sizes L of the CSYK with a box distribution are indicated by the black circles. The number of fermions is $N = L/2$ for even L and $N = (L + 1)/2$ for odd L . The r_s values expected for GOE (dashed red) GUE (dashed green) and GSE (dashed blue) are marked. The expected 4-fold symmetry is seen.

IV. LOCAL ENSEMBLE UNFOLDING

As discussed, the practice of determining the Thouless energy is fraught with difficulties. In order to compare any spectrum to RMT predictions, one must recast the spectrum such that it will exhibit an averaged constant density of states, i.e., a constant level spacing throughout the region examined. What is the averaging procedure? Usually, one averages the level spacing over an ensemble of disordered realizations in a given region and then reconstructs a particular spectrum such as the level spacing is on the average equal to 1 everywhere. Specifically, the averaged level spacing for the i -th level is $\Delta_i = \langle E_{i+m} - E_{i-m} \rangle / 2m$ (where m is $O(1)$, here chosen as $m = 5$), and the unfolded spectrum for the j -th realization is $\varepsilon_i^j = \varepsilon_{i-1}^j + (E_i^j - E_{i-1}^j) / \Delta_i$. For brevity we shall call this unfolding procedure local ensemble unfolding.

Implementation of this local unfolding procedure for the level number variance of CSYK with a box distribution and for a log-normal distribution $\gamma = 1, 1.5$ results in the behavior depicted in the inset of Fig 2, which is in agreement with the behavior observed in Refs. [6, 30]. Here the number variance begins by following the GOE predictions and grows quadratically for larger $\langle n \rangle$. The Thouless energy corresponds to the point where the number variance deviates from GOE predictions. As an estimate of the Thouless energy we chose the point for which the variance deviates by an arbitrary amount (set as 0.2), resulting in $E_{Th} \sim 95\Delta$, for the box distribution,

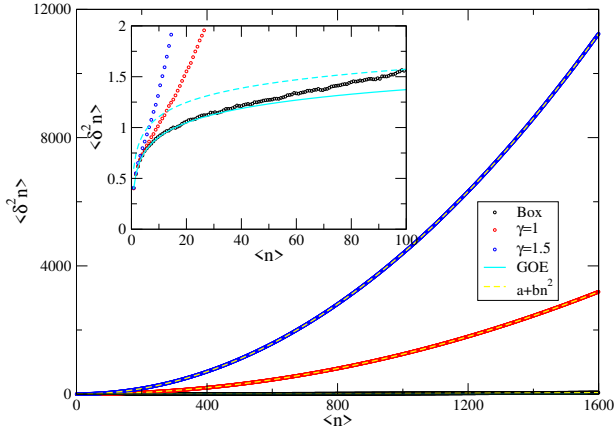


FIG. 2. The level number variance, $\langle \delta^2 n(E) \rangle$, as function of the energy window E . Symbols (black - box, red - $\gamma = 1$, blue $\gamma = 1.5$) represent the variance with local ensemble unfolding, fitted for larger values by $a + b\langle n(E) \rangle^2$ (where $b = 1.78 \cdot 10^{-5}$, for the box distribution, $b = 1.25 \cdot 10^{-3}$, for $\gamma = 1$, and $b = 4.4 \cdot 10^{-3}$, for $\gamma = 1.5$). The cyan line is the GOE prediction $\langle \delta^2 n(E) \rangle = (2/\pi^2) \ln(\langle n(E) \rangle) + 0.44$. Inset: zoom into smaller values of $\langle n \rangle$. Deviation from the GOE behavior are observed. A curve depicting GOE plus a constant of 0.2 corresponds the dashed cyan line. Using the intersection between the variance and the dashed cyan line to determine the Thouless energy results in $E_{Th} \sim 95\Delta$ for the box distribution, $E_{Th} \sim 13\Delta$, for $\gamma = 1$, and $E_{Th} \sim 7\Delta$ for $\gamma = 1.5$.

$E_{Th} \sim 13\Delta$, for $\gamma = 1$, and $E_{Th} \sim 7\Delta$ for $\gamma = 1.5$, where $\Delta = \langle \Delta_i \rangle$. This will naturally lead to the conclusion that as γ increases, E_{Th} strongly decreases. For larger values of γ the variance departs from the GOE predictions close to Δ and were not plotted to avoid cluttering the figure at small $\langle n \rangle$.

As emphasized by Jia and Verbaarschot [30], since unlike typical RMT models for which all non-diagonal terms are random, SYK models have just $\binom{2L}{4} \ll \binom{L}{N}$ independent non-diagonal terms, which leads to significant sample to sample fluctuations within the ensemble and using the average level spacing obtained by ensemble average may significantly skew the number variance. Thus, we need a way to characterize the level spacing for a specific sample. As previously discussed, in Ref. 30 this was achieved by parameterized the spectrum using Q-Hermite orthogonal polynomials. We will use the SVD method as described in the next section.

V. SINGULAR VALUE DECOMPOSITION

SVD can be used to characterize the features of the spectrum, for example on what scale does it follow RMT predictions [32–38]. For the analysis, one tabulates P

eigenvalues around the center of the band of M realizations of disorder as a matrix X of size $M \times P$ where X_{mp} is the p level of the m -th realization. The matrix X is decomposed to $X = U\Sigma V^T$, where U and V are $M \times M$ and $P \times P$ matrices correspondingly, and Σ is a diagonal matrix of size $M \times P$ and rank $r = \min(M, P)$. The r diagonal elements of Σ are the singular values amplitudes (SV) σ_k of X . All σ_k are positive and therefore may be ordered by their size $\sigma_1 \geq \sigma_2 \geq \dots \sigma_r$. The Hilbert-Schmidt norm of the matrix $\|X\|_{HS} = \sqrt{\text{Tr} X^\dagger X} = \sum_k \lambda_k$ (where $\lambda_k = \sigma_k^2$). The matrix X could be written as a series composed of matrices $X^{(k)}$, where $X_{ij}^{(k)} = U_{ik} V_{jk}^T$ and $X_{ij} = \sum_k \sigma_k X_{ij}^{(k)}$. This series in an approximation of matrix X , where the sum of the first m modes gives a matrix $\tilde{X} = \sum_{k=1}^m \sigma_k X^{(k)}$, for which $\|X\|_{HS} - \|\tilde{X}\|_{HS}$ is minimal.

The idea is that low modes capture the long-wavelength fluctuations of the spectrum, while higher modes sample the shorter wavelength fluctuations. If a distinct pattern of behavior of the amplitude as function of the mode number can be seen for a particular range of k , it is meaningful to discuss different behaviors at different energy scales. Indeed, examining the scree plot of the singular values λ_k for box distribution and log-normal distribution with different values of γ and a fixed $p = 0.5$, for $L = 16$, $N = 8$, with $M = 4096$ realizations and $P = 4096$ eigenvalues around the middle of the band one sees two distinct regions. The lowest modes ($k = 1, 2$ for box and $\gamma = 1$; $k = 1, 2, 3, 4$ for $1.5 \leq \gamma \leq 2.5$; and $k = 1, 2, 3, 4, 5, 6$ for $3 \leq \gamma \leq 5$) amplitudes are much larger than all the other modes, and determine the very long-wave behavior of the spectrum. The bulk of the modes for larger k follow a power-law behavior ($\lambda_k \sim k^{-\alpha}$) with $\alpha = 1$, as expected for Wigner-Dyson statistics [32–34].

In order to illustrate the difference between the local ensemble unfolding and unfolding using the lower modes of the SVD it is useful to examine the difference in the behavior of level spacing of the i -th level, Δ_i obtained by each method. While for the local ensemble unfolding the level spacing Δ_i is averaged over all realizations and therefore is not realization dependent, for the SVD unfolding the i -th level spacing of the j -th realization $\Delta_i^j = (\tilde{\varepsilon}_{i+m}^j - \tilde{\varepsilon}_{i-m}^j)/2m$, where $\tilde{\varepsilon}_i^j = \sum_{k=1}^2 \sigma_k U_{ik} V_{jk}^T$, is realization dependent. As can be seen in Fig. 4 there is a noticeable difference between the realization specific level spacing Δ_i^j and the ensemble average Δ_i . This difference becomes larger as γ increases, i.e., as the width of the log-normal distribution increases. Moreover, the difference, $\Delta_i^j - \Delta_i$, is long-range correlated for a given realization across thousands of levels. Thus, it makes sense to define the typical spacing difference between realizations $\delta\Delta = \sqrt{\langle (\Delta_i^j - \Delta_i)^2 \rangle_i}$. For $L = 16$, $N = 8$ with $M = 4096$ realizations and $P = 4096$ levels around the center of the band one gets $\delta\Delta = 4.44 \cdot 10^{-3}\Delta$ for the box distribution $\delta\Delta = 3.52 \cdot 10^{-2}\Delta$ for $\gamma = 1$ and $\delta\Delta = 6.61 \cdot 10^{-2}\Delta$ for $\gamma = 1.5$.

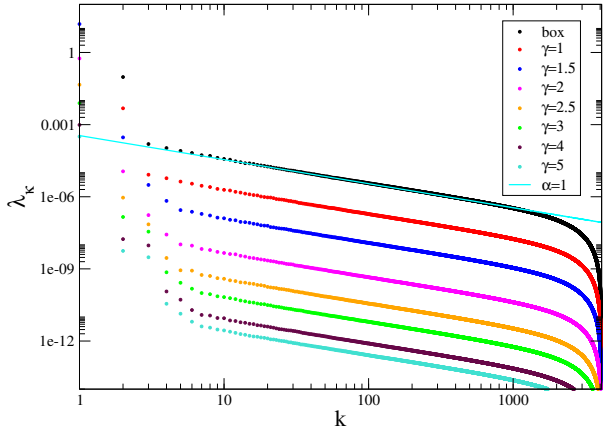


FIG. 3. The scree plot of the singular values for the CSYK with box and log-normal distribution with $p = 0.5$ and $\gamma = 1, 1.5, 2, 2.5, 3, 4, 5$ for $L = 16$, $N = 8$, with $M = 4096$ realizations and $P = 4096$ eigenvalues around the middle of the band. The square amplitude of the singular value λ_k are indicated by the symbols. The cyan line corresponds to $\lambda_k \sim k^{-\alpha}$, with $\alpha = 1$, as expected for a spectrum which follows Wigner-Dyson statistics. The lower k modes which capture the non-universal global structure of the spectrum deviate from Wigner-Dyson.

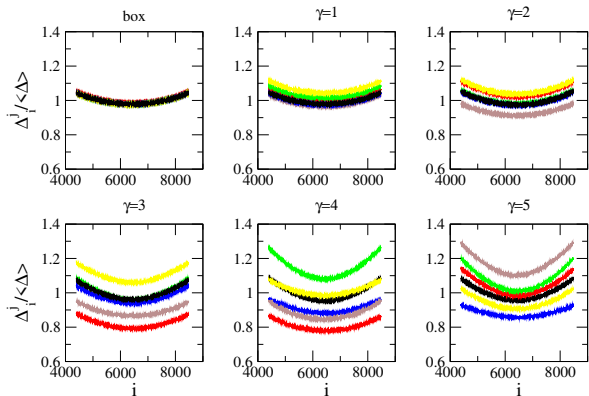


FIG. 4. The level spacing for the CSYK with box distribution and different log-normal distribution with $\gamma = 1, 2, 3, 4, 5$ for $L = 16$, $N = 8$, for $M = 4096$ realizations and $P = 4096$ eigenvalues around the middle of the band. The ensemble averaged level spacing, Δ_i , for the local unfolding method is the same for all samples and is depicted by the black curve. The SVD unfolded level spacing, Δ_i^j , is realization dependent. Five individual realizations for each distribution are shown (red, green, blue, yellow, brown curves). As γ increases the sample to sample fluctuations increases. It is clear that the long range correlations within a sample are very significant.

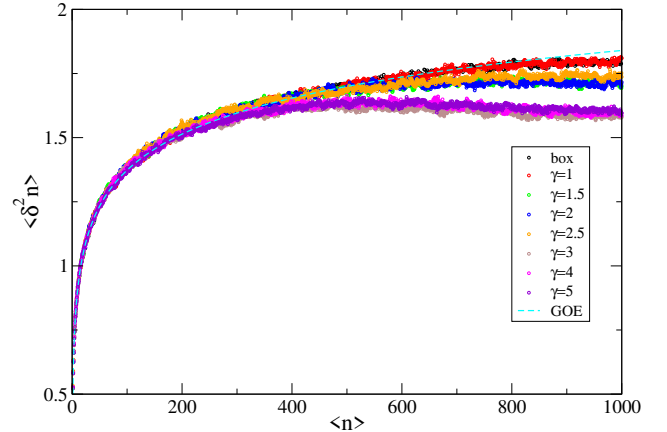


FIG. 5. The SVD unfolded level number variance, $\langle \delta^2 n(E) \rangle$, as function of the energy window E for box and log-normal $\gamma = 1, 1.5, 2, 2.5, 3, 4, 5$ represented by the symbols. The cyan dashed line is the GOE prediction $\langle \delta^2 n(E) \rangle = (2/\pi^2) \ln(\langle n(E) \rangle) + 0.44$. The SVD unfolded level number variance departs from GOE predictions at $E_{Th^*} \sim 800\Delta$ for the box and $\gamma = 1$ distributions, at $E_{Th^*} \sim 500\Delta$ for $1.5 \leq \gamma \leq 2.5$ distributions, and at $E_{Th^*} \sim 300\Delta$ for $3 \leq \gamma \leq 5$ distributions.

This long-range sample to sample level fluctuations can explain the behavior of the level number variance of the local ensemble unfolding seen in Fig. 3. Essentially, for larger values of $\langle n \rangle$, $\langle \delta^2 n \rangle = a + b \langle n \rangle^2$ with $b = 1.78 \cdot 10^{-5}$, for the box distribution, $b = 1.25 \cdot 10^{-3}$, for $\gamma = 1$, and $b = 4.4 \cdot 10^{-3}$, for $\gamma = 1.5$. The quadratic behavior could be understood as the consequence of realization specific long-range fluctuation of the level spacing. Calculating $\langle \delta^2 n \rangle = \langle (n - \langle n \rangle)^2 \rangle$, taking into account that after unfolding $\langle n \rangle = n$ and for a typical realization $n \sim n(1 + \delta\Delta/\Delta)$. Thus, $\langle \delta^2 n \rangle \sim (n\delta\Delta/\Delta)^2$, and after plugging in the above mentioned values of $\delta\Delta$ one obtains $\langle \delta^2 n \rangle \sim 1.97 \cdot 10^{-5} n^2$ for the box distribution, $\langle \delta^2 n \rangle \sim 1.24 \cdot 10^{-3} n^2$ for $\gamma = 1$ and $\langle \delta^2 n \rangle \sim 4.36 \cdot 10^{-5} n^2$ for $\gamma = 1.5$ in good agreement with the numerical value quoted above. Moreover, using our previous definition of the Thouless energy as the energy for which the deviation from RMT results becomes larger than some threshold, $b(E_{Th}/\Delta)^2 = 0.2$, and using $b = (\delta\Delta/\Delta)^2$, one gets $E_{Th} = 0.44\Delta^2/\delta\Delta$ resulting in $E_{Th} = 100\Delta, 18.5\Delta, 6.7\Delta$ for box and log-normal distributions with $\gamma = 1, 1.5$ correspondingly, in good agreement with the results in Fig. 3.

One concludes that the main contribution to the local ensemble average Thouless energy, E_{Th} , comes from the sample to sample long range fluctuations which can be quantified by $\delta\Delta$, the typical level spacing difference between the different realizations in the ensemble.

Thus, using the sample specific level spacing from the SVD (i.e., Δ_i^j) for unfolding will eliminate the sample

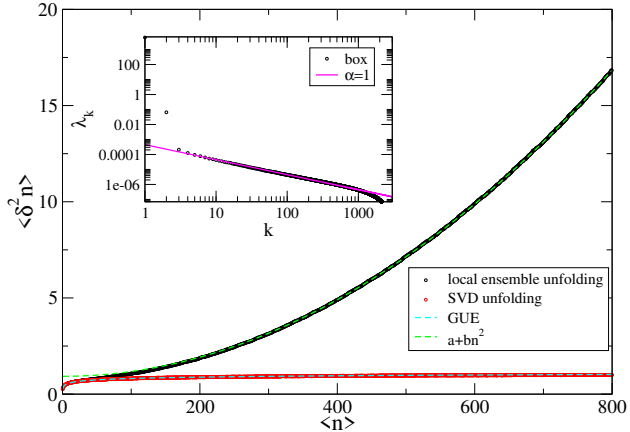


FIG. 6. The level number variance, $\langle \delta^2 n(E) \rangle$, as function of the energy window E for box distribution using local ensemble unfolding (black symbols) and SVD unfolding (red symbols) for $L = 15$, $N = 8$, $P = 3000$ and $M = 3000$. The cyan dashed line is the GUE prediction $\langle \delta^2 n(E) \rangle = (1/\pi^2) \ln(\langle n(E) \rangle) + 0.35$, while green dashed line follows $a + bn^2$ with $b = 2.48 \cdot 10^{-5}$. The different behavior for the two unfolding methods is clear. Inset: the scree plot of the singular value λ_k indicated by the symbols as function of k . The purple line corresponds to $\lambda_k \sim k^{-\alpha}$, with $\alpha = 1$.

to sample fluctuations contribution to the number variance. Indeed, using the SVD unfolded spectrum of the j -th realization $\tilde{\varepsilon}_i^j$ defined by $\varepsilon_i^j = \varepsilon_{i-1}^j + (\tilde{\varepsilon}_i^j - \tilde{\varepsilon}_{i-1}^j)/\Delta_i^j$, for the calculation of the realization specific level number variance one obtains the values depicted in Fig. 5. The number variance fits well with GOE expectations up to $E_{Th^*} \sim 800\Delta$ for the box and $\gamma = 1$ distributions, $E_{Th^*} \sim 500\Delta$ for $1.5 \leq \gamma \leq 2.5$ distributions, and $E_{Th^*} \sim 300\Delta$ for $3 \leq \gamma \leq 5$ distributions. The deviation is towards lower variance than predicted by GOE, similar to the behavior of the number variance after unfolding using Q-Hermite orthogonal polynomials [30]. As shown in Ref. 37 the energy of deviation from the universal behavior can be read off the scree plot by defining the mode for which the behavior deviates from the k^{-1} power law as k_{Th^*} . Thus, as can be garnered from Fig. 3, $k_{Th^*} \sim 2$ for the box and $\gamma = 1$ distributions, $k_{Th^*} \sim 4$ for $1.5 \leq \gamma \leq 2.5$ distributions, and $k_{Th^*} \sim 6$ for $3 \leq \gamma \leq 5$ distributions. Estimating the Thouless energy by $E_{Th^*} = r\Delta/2k_{Th^*}$ [37] results in $E_{Th^*} \sim 1000\Delta$, $E_{Th^*} \sim 500\Delta$, and $E_{Th^*} \sim 300\Delta$, not too far from the estimations obtained from Fig. 5.

Up to now we have mainly presented results for $L = 16$ which is the largest system for which we have ample statistics. Nevertheless, as can be seen in Fig. 1, for the CSYK the statistics changes for different values of L . In order to verify that our conclusions regarding the non-self-averaging behavior of the model are relevant for any symmetry, we calculated $\langle \delta^2 n(E) \rangle$ for the

box distribution using both local ensemble unfolding and SVD unfolding for $L = 15$, with $N = 8$ particles, for $P = 3000$ eigenvalues around the middle of the band for $M = 3000$ realizations. For this case GUE behavior, i.e., $\langle \delta^2 n(E) \rangle = (1/\pi^2) \ln(\langle n(E) \rangle) + 0.35$. Indeed, as can be seen in Fig. 6, both unfolding methods fit the GUE expectation for small $\langle n \rangle$. On larger scales the same difference that was seen for $L = 16$ GOE is seen for $L = 15$ GUE systems. The local ensemble unfolding results in $E_{Th} \sim 90\Delta$, and a fit to a quadratic behavior of the form $a + bn^2$ leads to $b = 2.48 \cdot 10^{-5}$, while for the SVD unfolding $E_{Th^*} \sim 800\Delta$. Comparing with the typical spacing difference between realizations for the box distribution which for $L = 15$ equals to $\delta\Delta = 5.17 \cdot 10^{-3}$, one would estimate $E_{Th} = 0.44\Delta^2/\delta\Delta \sim 85\Delta$ and $b = (\delta\Delta/\Delta)^2 \sim 2.67 \cdot 10^{-5}$, both in good agreement with the numerical results. As explained above for $E_{Th^*} = r\Delta/2k_{Th^*}$, and here $r = 3000$ and $k_{Th^*} \sim 2$, resulting in $E_{Th^*} \sim 750\Delta$, again in good agreement with the results.

VI. DISCUSSION

Much of the fascination with the SYK is connected to its chaotic behavior. Since short time scales are associated with large energy scales, deviation from GOE behavior of the spectra on large energy scales indicate non-chaotic behavior on short time scales. Estimating the time for which the chaotic behavior emerges is relevant to the estimation of the scrambling time of the SYK models, which motivates its application to studies of quantum gravity in black holes [41]. Ensemble averaging also plays an important role in the duality between SYK and classical general relativity.

For self-averaging systems there is no difference between averaging over the ensemble or averaging over a large single realization. As discussed, for finite size SYK samples, there is a huge difference between the Thouless time for a realization adjusted unfolding compared to the ensemble averaged unfolding, a difference which is larger as the distribution of the interaction elements is more skewed.

Nevertheless, it is relevant to extrapolate to infinite systems ($L \rightarrow \infty$) in order to see whether this difference persists. SYK has three time scales [42]: (i) band structure time t_B associated with the band width, B , (ii) Thouless time, t_{Th} or t_{Th^*} , on which much of the paper concentrated and (iii) Heisenberg time, t_H . Since the band width depends linearly on L [43], $t_B = \hbar/B \sim \hbar/L$. Thus, the Heisenberg time $t_H = \hbar/\Delta$ where $\Delta \sim B/2^L$, is $t_H = \hbar \cdot 2^L/L$. The Thouless time for the ensemble average is $t_{Th} = \hbar/E_{Th}$, where $E_{Th} \sim \Delta L^2$ and resulting in $t_{Th} = \hbar \cdot 2^L/L^3$. For the realization adjusted unfolding, $E_{Th^*} \sim 2^L \Delta B/k_{Th^*}$, with $k_{Th^*} \sim O(1)$, thus, $t_{Th^*} \sim k_{Th^*} \hbar/B \sim k_{Th^*}/L$. Hence, $t_H > t_{Th} \gg t_{Th^*} \geq t_B$, while the realization adjusted Thouless time $\lim_{L \rightarrow \infty} t_{Th^*} \rightarrow 0$, the ensemble averaged Thouless time $\lim_{L \rightarrow \infty} t_{Th} \rightarrow \infty$. The difference between t_{Th} and t_{Th^*}

increases as the distribution is more skewed (Figs. 2 and 5).

This leads to the conclusion that one can not determine the behavior of the SYK model by ensemble average for times shorter than t_{Th} since shorter times are non-self-averaging. Moreover, these shorter times ($t_{Th^*} \sim t_B < t < t_{Th}$) correspond to a parametrically large span of times. Therefore, when one wishes to study the transition from chaotic to localized behavior in mod-

ified SYK models [9–20] for which the number of independent random variables remain low, sample to sample fluctuations are expected to remain important and non-self-averaging at short times should be considered. In principal, although the transition occurs at long times nevertheless these effects could obscure the transition point and influence the perceived nature of the metallic regime. This will be considered in future studies.

-
- [1] S. Sachdev and J. Ye, Phys. Rev. Lett. **70**, 3339 (1993).
 [2] A. Kitaev, Talks at the KITP on April 7th and May 27th (2015).
 [3] S. Sachdev, Phys. Rev. X **5**, 041025 (2015).
 [4] J. Maldacena and D. Stanford, Phys. Rev. D **94**, 106002 (2016).
 [5] J. Maldacena, International journal of theoretical physics **38**, 1113 (1999).
 [6] A. M. García-García and J. J. M. Verbaarschot, Phys. Rev. D **94**, 126010 (2016).
 [7] Y-Z. You, A. W. W. Ludwig, and C. Xu, Phys. Rev. B **95**, 115150 (2017).
 [8] T. Li, J. Liu, Yuan Xin and Y. Zhou, J. High Energ. Phys. **06**, 111 (2017).
 [9] A. M. García-García, Y. Jia, and J. J. M. Verbaarschot, Phys. Rev. D **97**, 106003 (2018).
 [10] A. M. García-García, B. Loureiro, A. Romero-Bermúdez, and M. Tezuka, Phys. Rev. Lett. **120**, 241603 (2018).
 [11] T. Nosaka, D. Rosa, and J. Yoon, The Thouless time, J. High Energ. Phys. **06**, 41 (2018).
 [12] A. M. García-García and M. Tezuka, Phys. Rev. B **99**, 054202 (2019).
 [13] T. Micklitz, F. Monteiro, A. Altland, Phys. Rev. Lett. **123**, 125702 (2019).
 [14] F. Monteiro, M. Tezuka, A. Altland, D. A. Huse, T. Micklitz, Phys. Rev. Lett. **127**, 030601 (2021).
 [15] F. Monteiro, T. Micklitz, M. Tezuka, and A. Altland, Phys. Rev. Research **3**, 013023 (2021).
 [16] C.-M. Jian, Z. Bi, and C. Xu, Phys. Rev. B **96**, 115122 (2017).
 [17] S.-K. Jian and H. Yao, Phys. Rev. Lett. **119**, 206602 (2017).
 [18] X. Chen, R. Fan, Y. Chen, H. Zhai, and P. Zhang, Phys. Rev. Lett. **119**, 207603 (2017).
 [19] A. Altland, D. Bagrets, and A. Kamenev, Phys. Rev. Lett. **123**, 106601 (2019).
 [20] D. K. Nandy, T. Čadež, B. Dietz, A. Andreanov, and D. Rosa, arXiv:2206.08599.
 [21] M. L. Mehta, *Random matrices* (Acad. Press, New York, 1991), 2nd ed.
 [22] B. Shklovskii, B. Shapiro, B. R. Sears, P. Lambrianides and H. B. Shore, Phys. Rev. B. **47**, 11487 (1993).
 [23] T. Guhr, A. Muller-Groeling, H. A. Weidenmuller, Phys. Rep. **299**, 190 (1998).
 [24] Y. Alhassid, Rev. Mod. Phys. **72**, 895 (2000).
 [25] A.D. Mirlin, Phys. Rep. **326**, 259 (2000).
 [26] R. Evers and A.D. Mirlin, Rev. Mod. Phys. **80**, 1355 (2008).
 [27] B. Altshuler and B. Shklovskii, Sov. Phys. JETP [Zh. Eksp. Teor. Fiz. 91,220] **64**, 127 (1986).
 [28] J. Sonner and M. Vielma, J. High Energ. Phys. **11** 149 (2017).
 [29] A. Altland and D. Bagrets, Nucl. Phys. B **930**, 45 (2018).
 [30] Y. Jia and J. J.M. Verbaarschot, J. High Energ. Phys. **07** 193 (2020).
 [31] A. Aharony and A. Harris, Phys. Rev. Lett. **77**, 3700 (1996).
 [32] R. Fossion, G. Torres-Vargas and J. C. López-Vieyra, Phys. Rev. E, **88**, 060902(R) (2013).
 [33] G. Torres-Vargas, R. Fossion, C. Tapia-Ignacio and J. C. López-Vieyra, Phys. Rev. E, **96**, 012110 (2017).
 [34] G. Torres-Vargas, J. A. Méndez-Bermúdez, J. C. LópezVieyra and R. Fossion, Phys. Rev. E, **98**, 022110 (2018).
 [35] R. Berkovits, Phys. Rev. B **102**, 165140 (2020).
 [36] R. Berkovits, Phys. Rev. B **104**, 054207 (2021).
 [37] R. Berkovits, Phys. Rev. B **105**, 104203 (2022).
 [38] W.-J. Rao, Phys. Rev. B **105**, 054207 (2022).
 [39] I. M. Khaymovich, V. E. Kravtsov, B. L. Altshuler, and L. B. Ioffe, Phys. Rev. Res. **2**, 043346 (2020).
 [40] Y. Y. Atas, E. Bogomolny, O. Giraud, and G. Roux, Phys. Rev. Lett. **110**, 084101 (2013).
 [41] S. Sachdev, arXiv:2205.02285.
 [42] A. Altland, D. Bagrets, P. Nayak, J. Sonner, and M. Vielma, Phys. Rev. Res. **3**, 033259 (2021).
 [43] J. Cotler, G. Gur-Ari, M. Hanada, J. Polchinski, P. Saad, S. Shenker, D. Stanford, A. Streicher, and M. Tezuka, J. High Energ. Phys. **05**, 118 (2017).